nature chemistry

ARTICLES

PUBLISHED ONLINE: 22 AUGUST 2010 | DOI: 10.1038/NCHEM.803

Bridging-ligand-substitution strategy for the preparation of metal–organic polyhedra

Jian-Rong Li and Hong-Cai Zhou*

Metal–organic polyhedra—discrete molecular architectures constructed through the coordination of metal ions and organic linkers—have recently attracted considerable attention due to their intriguing structures, their potential for a variety of applications and their relevance to biological self-assembly. Several synthetic routes have been investigated to prepare these complexes. However, to date, these preparative methods have typically been based on the direct assembly of metal ions and organic linkers. Although these routes are convenient, it remains difficult to find suitable reaction conditions or to control the outcome of the assembly process. Here, we demonstrate a synthetic strategy based on the substitution of bridging ligands in soluble metal–organic polyhedra. The introduction of linkers with different properties from those of the initial metal–organic polyhedra can thus lead to new metal–organic polyhedra with distinct properties (including size and shape). Furthermore, partial substitution can also occur and form mixed-ligand species that may be difficult to access by means of other approaches.

The design and synthesis of supramolecular architectures based on coordination-driven self-assembly of relatively simple structural units has attracted considerable attention[1–13]. These supramolecular species not only have structural complexity, but also functionality in host–guest chemistry contexts. Their relevance in biological self-assembly as well as their impact on materials science are also significant.

In supramolecular coordination architectures, metal–organic polyhedra (MOPs) have attracted particular interest due to their well-defined and confined cavities, high symmetry and stability, and rich chemical and physical properties and functions[1–4,8,11]. In the past two decades, a large number of MOPs have been synthesized using a variety of strategies, including symmetry interaction, molecular library, directional bonding, supramolecular blueprint, molecular panelling, weak-link and reticular chemistry approaches[14–20]. These methods are all based on the spontaneous self-assembly of generally two, and in a few cases multiple, components in a given system. In this context, the steric, geometric and electronic characteristics embedded within individual components have collectively allowed the 'controllable' construction, to some extent, of 'designed' supramolecular entities.

Controllable coordination-driven self-assembly is most effective in a two-component assembly system. This restricts, to some extent, the diversity of the resulting assemblies because of limitations in the availability of components, particularly those with distinct geometries. In a multicomponent assembly, the formation of one or several products involves a series of component self-recognition/selection procedures under specific conditions[21–23]. Preparation and isolation of a particular desired product is therefore difficult due to the complexity of the multicomponent self-assembly process, although the formation and/or isolation of pure product has been demonstrated as a result of size selectivity or geometric cooperativity in rare cases[24,25].

In an alternative strategy, we show that multicomponent MOPs can be obtained by means of a partial bridging-ligand-substitution reaction carried out on existing MOPs. Part of the original structural and functional information can be preserved while some (but not all) of the bridging ligands are exchanged for alternative ligands of different sizes and shapes. Similarly, reversible substitution of all the bridging ligands can lead to interconversion between two supramolecular assemblies. Isolation of the resulting species as solid products can then be achieved based on their solubility in a given reaction solvent system. To the best of our knowledge, the bridging-ligand-substitution strategy has not yet been explored in the context of conversion and isolation of these complex discrete coordination architectures, although multicomponent assembly, dynamic interconversion and dynamic ligand exchange have been investigated in related systems[26–29].

Here, we present a bridging-ligand-substitution reaction as the synthetic strategy for the preparation and isolation of several novel MOPs based on a square four-connected $Cu_2(O_2CR)_4$ unit and various carboxylate ligands acting as building blocks (Fig. 1). One MOP is converted to another based on partial or complete bridging-ligand substitution of soluble MOP precursors. The resulting MOP compounds were isolated as crystalline products in each individual reaction system.

Results and discussion

The prerequisite for using the bridging-ligand-substitution strategy to synthesize new MOPs is that MOP precursors and new ligands should be soluble in the same solvent or solvent mixture. In this report, three soluble MOPs—$[Cu_{24}(\mathbf{A})_{24}(\mathbf{S})_{24}]\cdot x\mathbf{S}$ (**1**), $[Cu_{24}(\mathbf{B})_{24}(\mathbf{S})_{24}]\cdot x\mathbf{S}$ (**2**) and $Na_6H_{18}[Cu_{24}(\mathbf{C})_{24}(\mathbf{S})_{24}]\cdot x\mathbf{S}$ (**3**), where **S** represents a solvent molecule—were prepared as reactants for the ligand substitution reactions discussed above. The three MOPs were prepared by direct reaction of $Cu_2(OAc)_4\cdot H_2O$ and three angular di-acids: 5-*t*-butyl-1,3-benzenedicarboxylic acid H_2(5-*t*-Bu-1,3-BDC) (**A1**), where the symbol for the corresponding deprotonated form is designated as **A** (Fig. 1) (the other ligands and their corresponding acid forms have been designated similarly throughout this paper), 5-hydroxy-1,3-benzenedicarboxylic acid H_2(5-OH-1,3-BDC) (**B1**) and 5-sulfo-1,3-benzenedicarboxylic acid monosodium salt NaH_2(5-SO_3-1,3-BDC) (Na**C1**), respectively, at room temperature (Fig. 2).

MOP **1** is soluble in *N*,*N*-diethylformamide (DEF) and *N*-methylpyrrolidone (NMP), whereas **2** and **3** are soluble in MeOH. Each of the three compounds is stable in the solution of

Department of Chemistry, Texas A&M University, College Station, Texas 77842-3012, USA. *e-mail: zhouh@tamu.edu

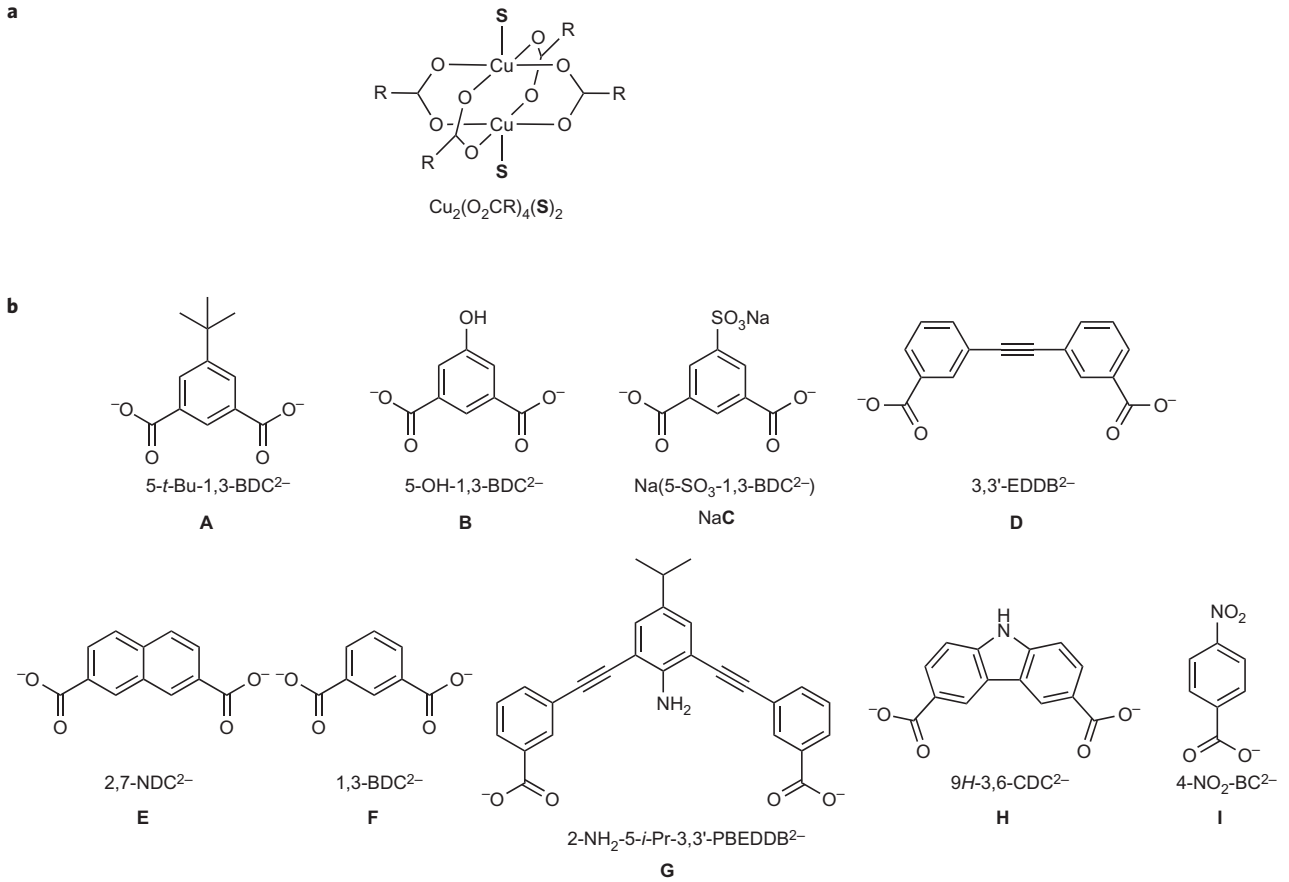

Figure 1 | Structures of the building blocks. a, Paddlewheel square four-connected dinuclear Cu_2 unit, in which R is an organic entity that extends the inorganic cluster to a complex architecture and **S** represents a coordinated terminal solvent molecule. **b**, Carboxylate ligands and their acronyms. All the ligands are designated by a bold letter from **A** to **I,** and their corresponding acid forms by **A1** to **I1**, respectively.

its respective solvent, but seems to decompose in the presence of water, as indicated in their absorption spectra (Supplementary Fig. S6). In addition, **3** is soluble in water, but decomposes in minutes to precipitate a white powder. The terminal groups of *t*-Bu, OH and SO_3^- in the three ligands are presumably responsible for the solubility of these compounds. Structurally, **1**–**3** have similar cuboctahedral geometries when the 12 Cu_2 units are viewed as vertices and ligands as edges. The structural descriptions of **1** and **2** have been reported[30,31]; the differences between the structures in this work and those described in the literature lie in the coordinated solvent molecules and the polymorphism in crystallization. Remarkably, **3** is an ionic MOP with 24 SO_3^- groups on the periphery. The SO_3^- groups should endow this MOP with potential in the construction of metal–organic frameworks (MOFs) as a MOP ligand through coordination with other metal ions.

Reaction of **1** with the newly synthesized 3,3′-(ethyne-1,2-diyl)-dibenzoic acid H_2(3,3′-EDDB) (**D1**) having a 60° bend angle in DEF gave a mixed-ligand MOP, $[Cu_{12}(\mathbf{A})_6(\mathbf{D})_6(\mathbf{S})_{12}]\cdot x\mathbf{S}$ (**4**), which was isolated as a crystalline product. X-ray diffraction revealed that **4** consisted of six **A** ligands, six **D** ligands and six Cu_2 units (Fig. 2). The structure can be described as two trigonal subunits, each of which comprises three **A** ligands and three Cu_2 units, linked through six **D** ligands to give a cage molecule with overall dimensions of ~25 × 28 Å and an internal elliptic cavity size of 7 × 13 Å (atom-to-atom distance after removing coordinated solvent molecules and considering van der Waals radii throughout this paper). When considering all organic ligands as edges and Cu_2 units as vertices, this cage has a distorted octahedral geometry with two types of triangular crevices measuring 4.0 × 4.0 × 4.0 Å and 4.0 × 5.5 × 5.5 Å (atom-to-atom distance along an edge determined after considering van der Waals radii, Fig. 3a). Compound **4** is a unique MOP constructed from two types of bridging angular ligands with bend angles of 60° and 120°, respectively. Metal-cluster-based MOPs with two types of angular bridging ligands are very rare; only two examples have been reported (very recently) from this research laboratory[25].

When **1** was reacted in DEF with 2,7-naphthalenedicarboxylic acid H_2(2,7-NDC) (**E1**), which has a 120° bend angle, another new MOP, $[Cu_{24}(\mathbf{A})_{12}(\mathbf{E})_{12}(\mathbf{S})_{24}]\cdot x\mathbf{S}$ (**5**), was obtained as single crystals. Structural analysis revealed that **5** is a quasi-spherical molecule consisting of 12 **A** ligands, 12 **E** ligands, and 12 Cu_2 paddlewheel units. It can also be viewed as four trigonal $(Cu_2)_3(\mathbf{A})_3$ subunits linked with four $(Cu_2)_3(\mathbf{E})_3$ subunits through the sharing of their edges (Fig. 2). The resulting polyhedron is similar to MOP **1**, with some distortion due to their being two types of ligands (Fig. 3b). The molecule has an approximate diameter of 32 Å and an internal cavity with a diameter of 15 Å. Two types of triangular windows are formed by three **A**- or three **E**-linked Cu_2 paddlewheel units, and one type of quadrangular window is observed in the structure. The sizes of these triangular and quadrangular windows are 4.0 × 4.0 × 4.0 Å, 6.2 × 6.2 × 6.2 Å and 4.0 × 6.2 × 4.0 × 6.2 Å, respectively. Compound **5** is unique among the MOPs because of the coexistence of two types of ligands that have the same bridging angle (120°) but different lengths. Additionally, it is interesting to note that the trigonal subunit constructed by the three **A** ligands and the three Cu_2 units from **1** is conserved in **4** and **5**, implying that such a fragment may be more favourable than others in the dynamic self-assembly procedure.

Similarly, **2** reacted with 1,3-benzenedicarboxylic acid H_2(1,3-BDC) (**F1**) in MeOH to give another mixed-ligand MOP,

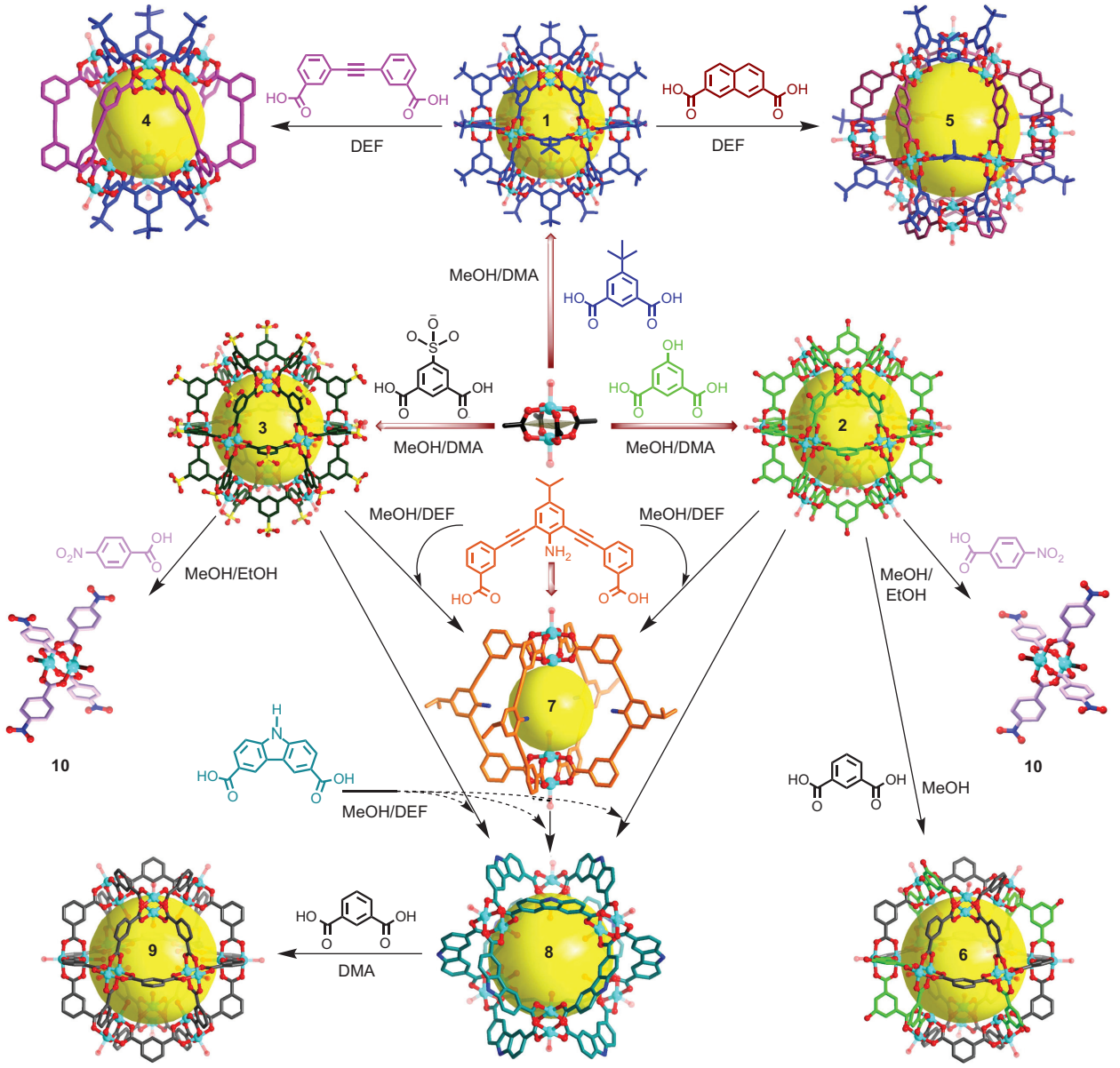

Figure 2 | Schematic of the syntheses and crystal structures of compounds 1–10. MOPs **1**–**3** were obtained by mixing $Cu_2(OAc)_4{\cdot}H_2O$ and the corresponding carboxylic acid ligands in a MeOH/DMA mixed solvent at room temperature. Compounds **4**–**10** were synthesized by mixing an excess amount of the acid form of the ligands with related soluble MOP starting materials in a suitable solvent at room temperature. After several days, single crystals were collected and characterized (DMA, *N*,*N*-dimethylacetamide; DEF, *N*,*N*-diethylformamide). In the structural views of **1**–**10**, all H atoms, uncoordinated solvent molecules, part atoms of coordinated terminal solvent molecules, and Na^+ ions in **3** have been omitted for clarity. Colour scheme for Cu atoms, cyan; for O atoms in MOPs **1**–**10**, red; for N atoms in **7** and **8**, blue; for S atoms in **3**, yellow; and for C atoms, the same colour as the corresponding ligands (all atoms in each ligand have the same colour, but different ligands have distinct colours) have been assigned in each MOP structure. The yellow sphere represents the free space inside each molecular cage.

$[Cu_{24}(\mathbf{B})_8(\mathbf{F})_{16}(\mathbf{S})_{24}]{\cdot}x\mathbf{S}$ (**6**), with a structure similar to that of **2** (Fig. 2). An X-ray diffraction study indicated the co-existence of **B** and **F** ligands in **6**, which are crystallographically disordered, making a precise assignment of the two ligands in the structure difficult. However, a ratio of about 1:2 of **B** and **F** was revealed by ^{1}H nuclear magnetic resonance (NMR) measurements of the ligand mixture from the degradation of **6** (Supplementary Fig. S1).

It should be pointed out that, in the formation processes of MOPs **4**–**6**, there are a multitude of oligomeric species in the reaction solution. The formation and isolation of **4**–**6** with mixed ligands can also be attributed partly to the geometric and steric cooperativity of participating ligands or subunits. If the geometries of two ligands are not compatible with one another, a single-ligand MOP will be isolated easily. For instance, in a MeOH/DEF mixed solvent, the reaction of **2** or **3** with another newly designed bridging ligand acid, 3,3′-(2-amino-5-*iso*-propyl-1,3-phenylene)*bis*(ethyne-2,1-diyl)dibenzoic acid H_2(2-NH_2-5-*i*-Pr-3,3′-PBEDDB) (**G1**), with a 'parallel' geometry (herein the bend angle can be viewed as '0°'), did not give a mixed-ligand MOP, but a single-ligand one, $[Cu_4(\mathbf{G})_4(\mathbf{S})_4]{\cdot}x\mathbf{S}$ (**7**). This molecule has a lantern-type structure comprising four ligands bridging two Cu_2 units, with a height of 18 Å and diameter of 29 Å, as well as an internal cavity of 5.2 × 9.5 Å (Fig. 2). It is interesting that the four NH_2 groups decorate the inner surface of this molecular cage, leading to potential utility in size-selective catalysis by using the basic NH_2 groups inside the cavity. In addition, the isopropyl group

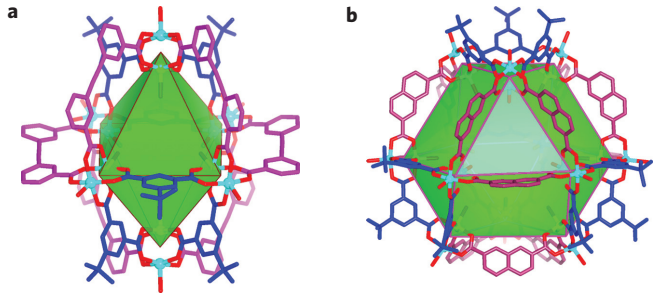

Figure 3 | Polyhedral representations of MOPs 4 and 5. a, Compound **4**. **b**, Compound **5**. The polyhedra were drawn by considering di-copper units as vertices and bridging ligands as edges. Metal clusters: Cu, cyan; O, red. All the C atoms of one ligand are shown in the same colour, but different ligands have distinct colours.

in the ligand makes **7** soluble in DEF, which allows it to react with other ligands in solution. The reaction of **7** with 9*H*-3,6-carbazole-dicarboxylic acid H_2(9*H*-3,6-CDC) (**H1**), which has a 90° bend angle, in MeOH/DEF also did not give a mixed-ligand MOP, but produced a single-ligand one, $[Cu_{12}(\mathbf{H})_{12}(\mathbf{S})_{12}]\cdot x\mathbf{S}$ (**8**) (Fig. 2). Similarly, **2** or **3** reacted with **H1** in a MeOH/DEF mixed solvent to also give **8**, but not a mixed-ligand MOP. MOP **8** has been reported recently by this laboratory[32], and is insoluble in MeOH but soluble in DMA and DEF. The solubility of **8** also allowed us to explore its reaction with **F1** in DMA, which gave another known MOP, $[Cu_{24}(\mathbf{F})_{24}(\mathbf{S})_{24}]\cdot x\mathbf{S}$ (**9**) (Fig. 2)[33,34]. Finally, a mono-topic carboxylic acid, 4-nitrobenzenecarboxylic acid H(4-NO_2-BC) (**I1**), terminated the formation of MOPs through a ligand substitution reaction with **2** or **3** in a MeOH/EtOH mixed solvent to give a simple dinuclear compound, $[Cu_2(\mathbf{I})_4(EtOH)_2]$ (**10**)[35].

We have therefore realized the conversion of one MOP to another based on a bridging-ligand-substitution reaction strategy. The versatility of this newly discovered synthetic strategy has also been demonstrated by the formation of a variety of MOPs. In particular, several novel MOPs with mixed ligands have been obtained as pure crystalline products. However, for the synthesis of mixed-ligand MOPs, a 'one-pot' reaction self-sorting approach (self-sorting: the mutual recognition of complementary components within a mixture[23], that is, the ability to efficiently distinguish self from non-self within complex mixtures during a self-assembly process) is also possible. For comparison, 'one-pot' reactions from mixed ligands and metal salts have also been performed for the synthesis of MOPs **4**–**6** (see Supplementary Information). Experiments have shown that under suitable conditions they can be obtained as crystals, together with an uncharacterized amorphous solid. Although the reaction conditions have not been optimized, the power of self-sorting cannot be underestimated, even in such a multicomponent self-assembly system. It also implies that the formation of such discrete polyhedral cages with mixed ligands is favoured thermodynamically or kinetically in the bridging-ligand-substitution reactions[36]. As demonstrated in the foregoing discussion, such a bridging-ligand-substitution synthetic strategy is generally applicable in the preparation of MOPs. It is also evident that the variation in solubility of these MOPs in different solvents or solvent combinations and the matching geometries of the bridging ligands lead to the isolation of pure crystalline product in each case.

It should be stressed that ligand substitution has long been used as a general synthetic strategy in inorganic and coordination chemistry[37–39]. A representative example is the substitution of carboxylate ligands on the periphery of the Mn_{12}-acetate single-molecule magnet, leading to a number of new Mn_{12} clusters[39]. When making comparisons with its use in other systems, the most distinct characteristic of the substitution reaction discussed herein is that the bridging ligands, which define the shape and size of a MOP, have been replaced, leading to MOPs with not only different compositions but also distinct sizes and geometric shapes. This is quite different from ligand substitutions in classic coordination complexes or the Mn_{12} clusters, in which molecular skeletons are usually preserved and the only change arises at the periphery of the molecules or clusters.

It is also important to contemplate the underlying reaction mechanism in this system on the basis of experimental observations, even though this may be very preliminary[40]. When considering the polygons formed by ligands linking the dimetal nodes and corresponding arrangements of ligands in a MOP, the 'polyhedral projection labelling' method could be proposed in studying the formation of these MOPs. In this work, two types of MOPs have been observed, with metal nodes being viewed as vertices and ligands as edges: the cuboctahedron found in MOPs **1**–**3**, **5**, **6** and **9**, and the octahedron associated with **4** and **8**. The cuboctahedrons include two types of polygonal windows that are trigonal and quadrangular in shape, respectively, whereas the octahedron has only triangular windows. The arrangements of ligands can thus be labelled in succession and linked to form new polygonal rings (3-, 4-, 6- or 8-membered rings), with each corner of each ring corresponding to one ligand. Starting from '1' at any corner of the top ring, the label increases by '1' clockwise until the ring is closed. Labelling continues to the closest corner of the next ring below until the bottom ring is fully labelled (Fig. 4). The cuboctahedral MOP therefore has two types of polyhedral projection arrays, [3,6,6,6,3]

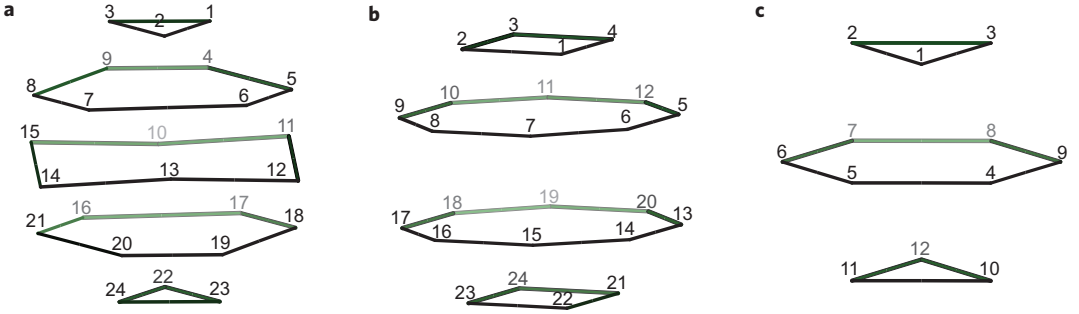

Figure 4 | Polyhedral projection labelling of MOPs. a,**b**, Cuboctahedral. **c**, Octahedral. The polyhedral projection labelling was proposed only to simplify the discussion in our attempts to analyse the underlying reaction mechanism in this system. Based on the positions and arrangements of bridging ligands in a MOP, each ligand is represented by a number and acts as a corner, which is linked across a di-copper node in succession to form a set of polygonal rings (3-, 4-, 6- or 8-membered rings). Projection from one of the windows formed by ligands bridging the di-copper units will give the corresponding polyhedral projection labelling array. Thus, for a cuboctahedral MOP, there exist two types of projection arrays, [3,6,6,6,3] (**a**) and [4,8,8,4] (**b**), whereas for an octahedral MOP, only one type is found, [3,6,3] (**c**).

(projected from one of the trigonal windows, Fig. 4a) and [4,8,8,4] (projected from one of the quadrangular windows, Fig. 4b), whereas the octahedral MOP only has a single projection array of [3,6,3] (Fig. 4c).

Based on the above simplification, in the formation of MOP **4** from the ligand substitution of **1**, the ligands in the two 3-membered rings were conserved (Fig. 4a), while those in all three 6-membered rings were substituted. Geometrically, the conversions of **2** or **3** to **8** as well as **8** to **9** are similar to that of **1** to **4**, with 3-membered ring units preserved but 6-membered ring units substituted. However, in the conversion of **1** to **5**, the situation becomes more complex: three ligands in the top 3-membered ring are conserved completely, and those in the first 6-membered ring (the second layer) are substituted completely. Half of the ligands (three) in the second 6-membered ring (the third layer) are substituted alternately, those in the third 6-membered ring (the fourth layer) are conserved completely, and the three ligands in the bottom 3-membered ring are substituted completely. Along the same lines, although the positions of two different types of ligands in **6** cannot be determined from X-ray structural analysis due to crystallographic disorder, based on the ratio of 1:2 of the two types of ligands, we can surmise that the ligand substitution of **2** to form **6** may occur according to the geometric positions shown in Fig. 4b, with all ligands in the two 4-membered rings conserved and those in the two 8-membered rings substituted completely. Although such an analysis seems arbitrary, the polyhedral projection labelling method can also be used conveniently in the analysis of other alternative substitution mechanisms.

Preliminary gas adsorption measurements of **1** were carried out at low temperatures. The results demonstrated the guest-evacuated **1** has the ability to selectively adsorb H_2 and O_2 over N_2 and Ar, and CO_2 over CH_4 (Fig. 5). It should be pointed out that the O_2 adsorption isotherm exhibits a two-step uptake at low pressure, and adsorption/desorption hysteresis loops were observed in the isotherms for all the gases tested (Supplementary Fig. S31). These phenomena, coupled with selective adsorption, can be attributed to the *t*-Bu groups in the MOP, which may partly block the windows of neighbouring molecular cages in the solid state, but are flexible due to weak van der Waals interactions[41]. Indeed, after guest removal, the sample became amorphous, as verified by powder X-ray diffraction (PXRD) (Supplementary Fig. S7). This may be attributed to the position rearrangement of the molecular cages of **1** with respect to one another upon activation. However, at the molecular level, the individual cage structure of **1** and thus its porosity should be maintained. It is unique for a MOP material showing selective gas adsorption. This type of material may consequently find application in gas separation and purification. Detailed investigations of the gas adsorption of all aforementioned MOPs, including the effects of coordinated terminal solvents and activation methods on the adsorption properties, will be reported elsewhere.

In summary, a bridging-ligand-substitution reaction strategy has been used successfully in the synthesis of MOPs with one or mixed ligands from soluble MOP precursors. By virtue of their insolubility in a given solvent or solvent mixture, the resulting novel MOPs can be isolated as pure crystalline products. In principle, by judiciously selecting a suitable solvent system, this method can be applied to the preparation of many novel MOPs. This general approach is also useful in constructing and isolating other complex metal–organic supramolecular architectures that may be difficult to access using the synthetic methods reported previously. Further work is being directed towards the design and synthesis of other angular ligands and their soluble coordination supramolecular entities, as well as their bridging-ligand-substitution reactions. These MOP materials may also play an important role in clean-energy-related gas separation, such as carbon dioxide capture, air separation and methane purification.

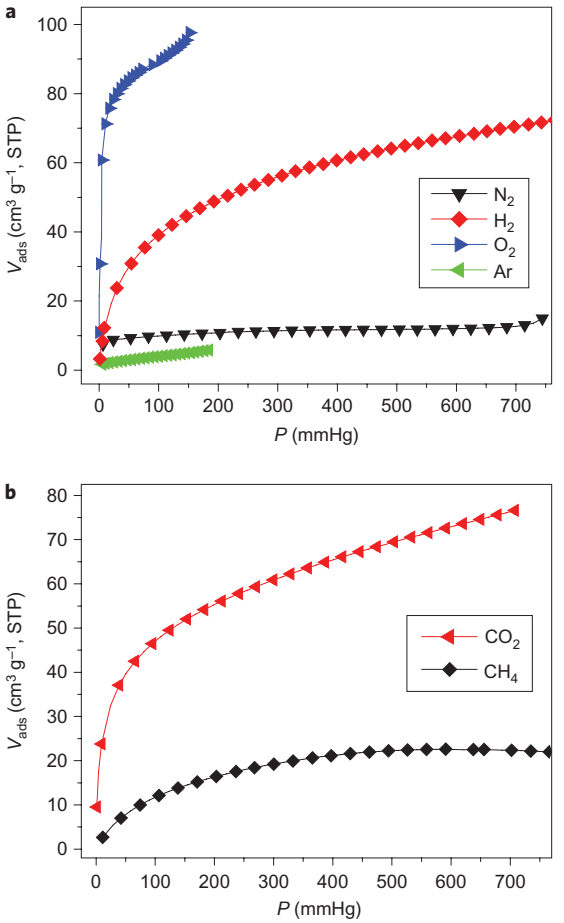

Figure 5 | Gas adsorption isotherms of activated MOP 1. a, N_2, H_2, O_2 and Ar adsorption isotherms measured at 77 K, showing selective adsorption of H_2 and O_2 over N_2 and Ar. **b**, CO_2 and CH_4 adsorption isotherms measured at 195 K, showing selective adsorption of CO_2 over CH_4.

Methods

Syntheses and reactions. 9*H*-3,6-Carbazoledicarboxylic acid H_2(9*H*-3,6-CDC) (**H1**) was synthesized according to a reported procedure[32]. 3,3′-(Ethyne-1,2-diyl)dibenzoic acid H_2(3,3′-EDDB) (**D1**) and 3,3′-(2-amino-5-*iso*-propyl-1,3-phenylene)*bis*(ethyne-2,1-diyl)dibenzoic acid H_2(2-NH_2-5-*i*-Pr-3,3′- PBEDDB) (**G1**) were newly designed and synthesized using palladium-catalysed Sonogashira coupling reactions. Compounds **1**–**3** were synthesized as crystals by the reaction of $Cu_2(OAc)_4{\cdot}H_2O$ with corresponding carboxylic acid ligands in a MeOH/DMA mixed solvent at room temperature. MOPs **4**–**10** were synthesized typically by mixing excess acid ligands with correlative soluble MOP starting materials in a suitable solvent at room temperature. After several days, the crystals were collected and structurally characterized. Phase purity of the products was evaluated by PXRD, and general characterizations including infrared, absorption spectra and thermogravimetric analysis (TGA) were carried out. Detailed descriptions of all syntheses and characterizations are given in the Supplementary Information.

X-ray single-crystal diffraction. Data were collected on a Bruker-AXS APEX-II charge-coupled device (CCD) diffractometer with a fine-focus sealed-tube X-ray source (Mo-K_α), and the structures were solved by direct methods. Details are provided in the Supplementary Information. In the crystal structure of **6**, two types of ligands, OH-1,3-BDC^{2-} and 1,3-BDC^{2-}, are of disordered distribution and a near 1:2 ratio was evaluated by ^{1}H NMR. Eight OH groups were refined in 16 positions, each having a 0.5 occupancy. In all the structures except **10**, solvent molecules and Na^+ ions in **3** were highly disordered, and attempts to locate and refine the solvent molecule and cation peaks were unsuccessful or imperfect. Diffused electron densities resulting from these solvent molecules (except the O atoms of coordinated solvents) or cations were removed from the data set using the SQUEEZE routine of PLATON and refined further using the data generated[42]. For the coordinated solvents, only O atoms were left and refined. The contents of the removed solvent region and cations (in **3**) are not represented in the unit cell contents in the crystal data of **1**–**9**. Attempts to determine the final formulae of these compounds from the SQUEEZE results combined with elemental analysis and TGA data were not

successful because of the volatility of the crystallization solvents during measurements; therefore, an accurate data set could not be obtained. Crystallographic data have been deposited with the Cambridge Crystallographic Data Centre: CCDC 755921 (MOP **1**); CCDC 755922 (MOP **2**); CCDC 755923 (MOP **3**); CCDC 755924 (MOP **4**); CCDC 755925 (MOP **5**); CCDC 755926 (MOP **6**); CCDC 755927 (MOP **7**); CCDC 755928 (MOP **8**); CCDC 755929 (MOP **9**); CCDC 755930 (MOP **10**). These data can be obtained free of charge from The Cambridge Crystallographic Data Center via www.ccdc.cam.ac.uk/data_request/cif.

Adsorption measurements. Gas adsorption measurements were performed using an ASAP 2020 volumetric adsorption analyser. Before adsorption, the sample was activated by solvent exchange followed by degassing as detailed in the Supplementary Information.

Received 2 February 2010; accepted 13 July 2010; published online 22 August 2010

References

1. Olenyuk, B., Whiteford, J. A., Fechtenkötter, A. & Stang, P. J. Self-assembly of nanoscale cuboctahedra by coordination chemistry. *Nature* **398,** 796–799 (1999).
2. Takeda, N., Umemoto, K., Yamaguchi, K. & Fujita, M. A nanometre-sized hexahedral coordination capsule assembled from 24 components. *Nature* **398,** 794–796 (1999).
3. Hof, F. & Rebek, J. Jr. Molecules within molecules: recognition through self-assembly. *Proc. Natl Acad. Sci. USA* **99,** 4775–4777 (2002).
4. Pluth, M. D., Bergman, R. G. & Raymond, K. N. Acid catalysis in basic solution: a supramolecular host promotes orthoformate hydrolysis. *Science* **316,** 85–88 (2007).
5. Lehn, J.-M. From supramolecular chemistry towards constitutional dynamic chemistry and adaptive chemistry. *Chem. Soc. Rev.* **36,** 151–160 (2007).
6. Koblenz, T. S., Wassenaar, J. & Reek, J. N. H. Reactivity within a confined self-assembled nanospace. *Chem. Soc. Rev.* **37,** 247–262 (2008).
7. Lee, S. J. *et al.* Cavity-tailored, self-sorting supramolecular catalytic boxes for selective oxidation. *J. Am. Chem. Soc.* **130,** 16828–16829 (2008).
8. Jung, M., Kim, H., Baek, K. & Kim, K. Synthetic ion channel based on metal–organic polyhedra. *Angew. Chem. Int. Ed.* **47,** 5755–5757 (2008).
9. Mal, P., Breiner, B., Rissanen, K. & Nitschke, J. R. White phosphorus is air-stable within a self-assembled tetrahedral capsule. *Science* **324,** 1697–1699 (2009).
10. Sawada, T., Yoshizawa, M., Sato, S. & Fujita, M. Minimal nucleotide duplex formation in water through enclathration in self-assembled hosts. *Nature Chem.* **1,** 53–56 (2009).
11. Ronson, T. K. *et al.* Stellated polyhedral assembly of a topologically complicated $Pd_4\mathbf{L}_4$ 'Solomon cube'. *Nature Chem.* **1,** 212–216 (2009).
12. Stoddart, J. F. Thither supramolecular chemistry. *Nature Chem.* **1,** 14–15 (2009).
13. Duriska, M. B. *et al.* Systematic metal variation and solvent and hydrogen-gas storage in supramolecular nanoballs. *Angew. Chem. Int. Ed.* **48,** 8919–8922 (2009).
14. Caulder, D. L. & Raymond, K. N. Supermolecules by design. *Acc. Chem. Res.* **32,** 975–982 (1999).
15. Leininger, S., Olenyuk, B. & Stang, P. J. Self-assembly of discrete cyclic nanostructures mediated by transition metals. *Chem. Rev.* **100,** 853–908 (2000).
16. Fujita, M. *et al.* Molecular paneling via coordination. *Chem. Commun.* 509–518 (2001).
17. McKinlay, R. M., Cave, G. W. V. & Atwood, J. L. Supramolecular blueprint approach to metal-coordinated capsules. *Proc. Natl Acad. Sci. USA* **102,** 5944–5948 (2005).
18. Gianneschi, N. C., Maser, M. S. & Mirkin, C. A. Development of a coordination chemistry-based approach for functional supramolecular structures. *Acc. Chem. Res.* **38,** 825–837 (2005).
19. Tranchemontagne, D. J., Ni, Z., O'Keeffe, M. & Yaghi, O. M. Reticular chemistry of metal–organic polyhedra. *Angew. Chem. Int. Ed.* **47,** 5136–5147 (2008).
20. Hamilton, T. D., Papaefstathiou, G. S., Friščić, T., Bučar, D.-K. & MacGillivray, L. R. Onion-shell metal–organic polyhedra (MOPs): a general approach to decorate the exteriors of MOPs using principles of supramolecular chemistry. *J. Am. Chem. Soc.* **130,** 14366–14367 (2008).
21. Ercolani, G. Assessment of cooperativity in self-assembly. *J. Am. Chem. Soc.* **125,** 16097–16103 (2003).
22. Nitschke, J. R. & Lehn, J.-M. Self-organization by selection: generation of a metallosupramolecular grid architecture by selection of components in a dynamic library of ligands. *Proc. Natl Acad. Sci. USA* **100,** 11970–11974 (2003).
23. Zheng, Y.-R., Yang, H.-B., Northrop, B. H., Ghosh, K. & Stang, P. J. Size selective self-sorting in coordination-driven self-assembly of finite ensembles. *Inorg. Chem.* **47,** 4706–4711 (2008).
24. Northrop, B. H., Zheng, Y.-R., Chi, K.-W. & Stang, P. J. Self-organization in coordination-driven self-assembly. *Acc. Chem. Res.* **42,** 1554–1563 (2009).
25. Li, J.-R. & Zhou, H.-C. Metal–organic hendecahedra assembled from dinuclear paddlewheel nodes and mixtures of ditopic linkers with 120 and 90° bend angles. *Angew. Chem. Int. Ed.* **48,** 8465–8468 (2009).
26. Fujita, M., Fujita, N., Ogura, K. & Yamaguchik, K. Spontaneous assembly of ten components into two interlocked, identical coordination cages. *Nature* **400,** 52–55 (1999).
27. Hiraoka, S., Sakata, Y. & Shionoya, M. Ti(IV)-centered dynamic interconversion between Pd(II), Ti(IV)-containing ring and cage molecules. *J. Am. Chem. Soc.* **130,** 10058–10059 (2008).
28. Al-Rasbi, N. K. *et al.* Mixed-ligand molecular paneling: dodecanuclear cuboctahedral coordination cages based on a combination of edge-bridging and face-capping ligands. *J. Am. Chem. Soc.* **130,** 11641–11649 (2008).
29. Zheng, Y.-R. & Stang, P. J. Direct and quantitative characterization of dynamic ligand exchange between coordination-driven self-assembled supramolecular polygons. *J. Am. Chem. Soc.* **131,** 3487–3489 (2009).
30. Ke, Y., Collins, D. J. & Zhou, H.-C. Synthesis and structure of cuboctahedral and anticuboctahedral cages containing 12 quadruply bonded dimolybdenum units. *Inorg. Chem.* **44,** 4154–4156 (2005).
31. Abourahma, H. *et al.* Hydroxylated nanoballs: synthesis, crystal structure, solubility and crystallization on surfaces. *Chem. Commun.* 2380–2381 (2001).
32. Li, J.-R., Timmons, D. J. & Zhou, H.-C. Interconversion between molecular polyhedra and metal–organic frameworks. *J. Am. Chem. Soc.* **131,** 6368–6369 (2009).
33. Eddaoudi, M. *et al.* Porous metal–organic polyhedra: 25 Å cuboctahedron constructed from 12 $Cu_2(CO_2)_4$ paddle-wheel building blocks. *J. Am. Chem. Soc.* **123,** 4368–4369 (2001).
34. Moulton, B., Lu, J., Mondal, A. & Zaworotko, M. J. Nanoballs: nanoscale faceted polyhedra with large windows and cavities. *Chem. Commun.* 863–864 (2001).
35. Kristiansson, O. & Tergenius, L.-E. Structure and host–guest properties of the nanoporous diaquatetrakis(p-nitrobenzoato)dicopper(II) framework. *J. Chem. Soc. Dalton Trans.* 1415–1420 (2001).
36. Sato, S., Ishido, Y. & Fujita, M. Remarkable stabilization of $M_{12}\mathbf{L}_{24}$ spherical frameworks through the cooperation of 48 Pd(II)–pyridine interactions. *J. Am. Chem. Soc.* **131,** 6064–6065 (2009).
37. Richens, D. T. Ligand substitution reactions at inorganic centers. *Chem. Rev.* **105,** 1961–2002 (2005).
38. Puddephatt, R. J. Macrocycles, catenanes, oligomers and polymers in gold chemistry. *Chem. Soc. Rev.* **37,** 2012–2027 (2008).
39. Bagai, R. & Christou, G. The *Drosophila* of single-molecule magnetism: $[Mn_{12}O_{12}(O_2CR)_{16}(H_2O)_4]$. *Chem. Soc. Rev.* **38,** 1011–1026 (2009).
40. Larsen, R. W. How fast do metal organic polyhedra form in solution? Kinetics of $[Cu_2(5\text{-OH-bdc})_2\mathbf{L}_2]_{12}$ formation in methanol. *J. Am. Chem. Soc.* **130,** 11246–11247 (2008).
41. Tozawa, T. *et al.* Porous organic cages. *Nature Mater.* **8,** 973–978 (2009).
42. Spek, A. L. Single-crystal structure validation with the program PLATON. *J. Appl. Crystallogr.* **36,** 7–13 (2003).

Acknowledgements

This material is based upon work supported as part of the Center for Gas Separations Relevant to Clean Energy Technologies, an Energy Frontier Research Center funded by the U.S. Department of Energy, Office of Science, Office of Basic Energy Sciences under award no. DE-SC0001015. The authors thank A. Yakovenko for his help in crystal structure refinement and PXRD analysis.

Author contributions

J.R.L. and H.C.Z. conceived and designed the experiments, analysed data and co-wrote the paper. J.R.L. performed all experiments.

Additional information

The authors declare no competing financial interests. Supplementary information and chemical compound information accompany this paper at www.nature.com/naturechemistry. Reprints and permission information is available online at http://npg.nature.com/reprintsandpermissions/. Correspondence and requests for materials should be addressed to H.C.Z.